Published in final edited form as:
Mol Cancer Res. 2014 September ; 12(9): 1244–1253. doi:10.1158/1541-7786.MCR-14-0223-T.

SIRT2 Interacts with β-catenin to Inhibit Wnt Signaling Output in Response to Radiation-Induced Stress

Phuongmai Nguyen[1], **Sunmin Lee**[2], **Dominique Lorang-Leins**[1], **Jane Trepel**[2], and **DeeDee K. Smart**[1]

[1]Radiation Oncology Branch, National Cancer Institute, National Institutes of Health, Bethesda, MD

[2]Medical Oncology Branch, National Cancer Institute, National Institutes of Health, Bethesda, MD

Abstract

Wnt signaling is critical to maintaining cellular homeostasis via regulation of cell division, mitigation of cell stress, and degradation. Aberrations in Wnt signaling contribute to carcinogenesis and metastasis, while sirtuins have purported roles in carcinogenesis, aging, and neurodegeneration. Therefore, the hypothesis that sirtuin 2 (SIRT2) directly interacts with β-catenin was tested and whether this interaction alters the expression of Wnt target genes to produce an altered cellular phenotype. Co-immunoprecipitation studies, using mouse embryonic fibroblasts (MEFs) from Sirt2 wild-type and genomic knockout mice, demonstrate that β-catenin directly binds SIRT2. Moreover, this interaction increases in response to oxidative stress induced by ionizing radiation (IR). Additionally, this association inhibits the expression of important Wnt target genes like survivin (BIRC5), cyclin D1 (CCND1), and c-myc (MYC). In Sirt2 null MEFs, an up-regulation of matrix metalloproteinase 9 (MMP9) and decreased E-cadherin (CDH1) expression is observed that produces increased cellular migration and invasion. Together, these data demonstrate that SIRT2, a tumor suppressor lost in multiple cancers, inhibits the Wnt signaling pathway in non-malignant cells by binding to β-catenin and that SIRT2 plays a critical role in the response to oxidative stress from radiation.

Keywords

SIRT2; β-catenin; Wnt Signaling; Gene Expression; Radiation

Introduction

The Wnt signaling pathway is crucial in regulating cell proliferation, apoptosis, migration and differentiation (1). β-catenin is a critical co-activator of Wnt-mediated gene expression. When Wnt ligands are present, β-catenin accumulates in the cytoplasm and is transported to the nucleus whereupon it binds to the lymphocyte enhancer factor (LEF)/T cell factor (TCF) complex to recruit chromatin remodeling complexes and activates gene expression (2–4).

Corresponding author: DeeDee K. Smart, M.D., Ph.D., Radiation Oncology Branch, National Cancer Institute, National Institutes of Health, 9000 Rockville Pike, Bethesda, MD 20892, Tel. (301) 496-5457, smartd@mail.nih.gov.

The authors disclose no potential conflicts of interest.

Disruptions of Wnt signaling are associated with accelerated aging (5, 6) and abnormal neural development (7) as well as several major diseases including schizophrenia, autism, Alzheimer's disease and cardiovascular disease (3, 8, 9). Additionally, aberrant regulation of β-catenin pathway has been shown to promote tumorigenesis including colon, breast, prostate, ovary and melanoma cancers (10).

Sirtuin 2 (SIRT2) belongs to the family of sirtuins which are NAD+-dependent class III protein deacetylases, and have been shown to play a major role in metabolism and longevity. SIRT2 expresses mainly in the brain, particularly the hippocampus and oligodendrocytes. SIRT2 is reported to deacetylate α-tubulin, thereby regulating microtubule dynamics. Consequently, SIRT2 is proposed to play a role in mitotic checkpoint to maintain genomic integrity (11–13). It has also been observed that SIRT2 may act as a tumor suppressor since SIRT2 is down-regulated in gliomas (14), while high levels of SIRT2 in tumors confers resistance to chemotherapy (15). In the central nervous system, SIRT2 is believed to participate in oligodendrocyte differentiation (16), and SIRT2 has been found to accumulate in the aging rodent brain (17).

In this study we show that SIRT2 directly interacts with β-catenin, and the interaction increases following IR exposure. Genetic deletion of *Sirt2* leads to activation of Wnt target genes such as *c-myc*, *cyclin D1* and *survivin*. Furthermore, we observe that SIRT2 is critical for regulating cell migration through induction of matrix metalloproteinase 9 (MMP-9) and down-regulation of E-cadherin. These findings provide a mechanistic insight into SIRT2 as a potential tumor suppressor and in cellular response to IR-induced oxidative stress in non-transformed cells. Furthermore, MMP9 and E-cadherin may potentially act as molecular markers for cells lacking *Sirt2* in regulating cell migration/invasion.

MATERIALS AND METHODS

Cell Culture, Radiation Exposure and Clonogenic Survival Assay

Primary mouse embryonic fibroblasts (MEFs) derived from wild type and *Sirt2* knockout mice [background C57B (60%)/C129 (40%)], a kind gift of Dr. Hyun-Seok Kim and Dr. Chu-Xia Deng (NIH) in 2011, were immortalized and described previously (18). As the cells were previously characterized, we did not perform further testing or authentication. MEFs were cultured in DMEM supplemented with 1% penicillin -streptomycin, 15% fetal bovine serum and 1% non-essential amino acid (Invitrogen). Cells that were passage greater than 37 were used in all experiments. PC-3 and U87 cells were obtained from ATCC in 2011 and authenticated by STR analysis upon purchase prior to preservation. Cells were passaged within 4 months of resuscitation according to the ATCC protocol and routinely tested for Mycoplasma infection using MycoAlert™ Mycoplasma Detection Kit (Lonza).

Mouse *Sirt2* shRNA (Origene) was electroporated into *Sirt2* WT MEFs using Amaxa Nucleofector kit (Lonza). Colonies were selected in 3μg/ml puromycin, and colonies with decreased SIRT2 expression were screened by immunoblot. Human Flag-*SIRT2* (Addgene) was electroporated into U87 glioma cells. Stable transfectants were selected in G-418, and positive clones were screened by immunoblot with anti-Flag antibody (Origene).

Cells were exposed to IR in an X-Rad 320 biological irradiator (Precision X-ray, Inc.), at a dose rate of 2.1 Gy/min.

To determine radiosensitivity, cells were plated at clonal density and irradiated 6h after plating. Experiments were terminated when visible colonies (>50 cells/colony) were present. Cells were stained with 0.5% crystal violet, the number of colonies counted and the surviving fractions were calculated and normalized to unirradiated controls respectively.

Antibodies

The following antibodies were purchased: SIRT2 (Sigma), β-catenin, cyclin D1, c-jun and survivin (Santa Cruz), phospho-β-catenin Y142 (Abcam), GSK3β and pGSK3β (BD Biosciences), acetylated lysine, acetylated β-catenin, MMP-9, E-cadherin, Akt, pAkt (Ser473) and c-myc (Cell Signaling).

Subcellular Fractionation

Cells were subjected to subcellular fractionation using NE-PER Nuclear and Cytoplasmic Extraction Reagents kit (Thermo Scientific). Band intensities from subcellular fractionation experiments were quantified using ImageQuant software (GE Healthcare). Relative fold change was determined by dividing band intensities of cytoplasmic β-catenin and nuclear β-catenin into band intensities of manganese SOD2 and lamin B respectively.

Immunofluorescence Microscopy

Immunofluorescent staining was performed as previously described (19). Photographs were taken with a 63X oil immersion objective.

Co-immunoprecipitation and Immunoblot

Cells were lysed in TNN (50mM Tris-HCl, pH 8.0, 120mM NaCl, 1% NP-40) buffer for immunoprecipitation experiments or in RIPA buffer (Thermo Scientific) for immunoblot analysis as previously described (20).

Measurement of Intracellular Reactive Oxygen Species (ROS)

Intracellular ROS quantification was carried out as described by Slane et al (21). Briefly, *Sirt2* WT and KO MEFs were labeled with either carboxy-DCFDA or H_2DCFDA (Invitrogen). After incubation for 30 min at 37°C, the dye was removed, and cells received either sham or 10 Gy radiation. Thirty minutes after exposure, the fluorescent intensity was measured. H2DCFDA: DCFDA ratio was calculated, normalized to either *Sirt2* WT or KO control, respectively, and presented as normalized fluorescent intensity. To inhibit ROS generated by radiation, cells were pretreated with 200 U/ml PEG-catalase (Sigma) for 2h prior to labeling the cells. PEG-catalase treatment continued throughout the labeling and radiation exposure.

In Vitro Deacetylation Assay of β-catenin

In vitro deacetylation was performed as described by Zhang et al. (22). Briefly, *Sirt2* KO MEFs were lysed in TNN buffer and 1 mg of cell lysates were used to immunoprecipitate β-

catenin. Immunoprecipitates were resuspended in the presence or absence of purified recombinant human SIRT2 (BPS Bioscience) with or without NAD+. The reaction was stopped and samples analyzed by immunoblot with antibodies against acetylated lysine, β-catenin or SIRT2.

RNA Extraction and Real-Time PCR

RNA was isolated using an RNeasy Mini kit (Qiagen), and reverse transcription and real-time PCR were carried out as previously described (23). Wnt pathway PCR Array and reagents were from Qiagen. Primers used for RT-PCR are shown in Supplementary Table S1.

pTOPFLASH Reporter Assays

Sirt2 WT and KO MEFs were co-transfected with 1.5 μg of pTOPFLASH luciferase reporter, which contains four TCF-responsive elements in tandem, or pGL2-Basic empty vector and 150 ng of β-galactosidase expression plasmid (pCMV-β-gal) using FuGENE 6 (Roche Diagnostics). Total amount of luciferase and β-galactosidase activities were measured And relative fold induction of luciferase activity was normalized to β-galactosidase activity. The results are represented as ratio of pTOPFLASH-luciferase over empty vector pGL2.

Cell Invasion Assay

Cell culture inserts with an 8-μm pore-size PET membrane (Fisher Scientific) were coated with collagen IV (Becton-Dickinson) and placed into 24-well plates containing 0.5 ml of DMEM medium supplemented with 15% FBS. 6.25×10^3 cells in serum-free DMEM were plated into the inserts and incubated for 18 h at 37°C. Cells from the upper surface of the membrane were then removed and the remaining cells adhered to the bottom of the membrane were Wright stained (Fisher Scientific). Six random fields per membrane were photographed at 40X and counted.

Chromatin Immunoprecipitation (ChIP)

ChIP assays were carried out as described previously (20). Purified DNA samples were analyzed by real-time quantitative PCR using SYBR Green PCR Master Mix (Applied Biosystems) with primers to the promoters of *Myc*, *cyclin D1* and *survivin* (Supplementary Table S1).

Statistical Analyses

Unless indicated otherwise, all observations were confirmed by at least three independent experiments. The results are presented as the mean ± SEM. We used two-tailed Student *t* tests as determined by GraphPad Prism software (La Jolla, CA) for statistical analysis. P values < 0.05 was considered as statistically significant.

RESULTS

Nuclear β-Catenin Level Is Elevated in Sirt2 KO MEFs

Since transcriptionally active β-catenin accumulates in the nucleus, we first determined the subcellular localization of β-catenin in wild-type (WT) *Sirt2* MEFs compared to knock-out (KO) *Sirt2* MEFs generated through genomic deletion. Using lamin B as a nuclear marker and manganese superoxide dismutase as a cytoplasmic marker, we demonstrate by immunoblot analysis of nuclear- and cytoplasmic-enriched fractions that there is a significant increase in nuclear β-catenin protein present in the *Sirt2* KO MEFs relative to WT (Fig. 1A). This increase is greater than two-fold as analyzed by densitometry (Fig. 1B, columns 1& 2). Conversely, there is a corresponding increase of cytoplasmic β-catenin present in the *Sirt2* WT MEFs (Fig. 1A) compared to KO; this increase is also greater than two-fold as determined by densitometry (Fig. 1B, columns 3 & 4). Total β-catenin protein level remains constant between the 2 cell types (Fig. 1D).

Immunofluorescence analysis of *Sirt2* WT and KO cells using β-catenin antibody shows that roughly 70% of the *Sirt2* KO cells observed have strong immunoreactivity in the nucleus with weak but detectable immunoreactivity in the cytoplasm (Fig. 1C). In contrast, less than 5% of the *Sirt2* WT fibroblasts showed strong nuclear β-catenin staining, while the majority exhibited low nuclear reactivity for β-catenin. Immunofluorescent staining provides additional data to demonstrate a stronger nuclear β-catenin presence in the *Sirt2* KO cells. This is probably due to the fact that not all the *Sirt2* KO cells have increased β-catenin nuclear localization and thus may have diluted out during the subcellular fractionation procedure.

Previous studies have shown that phosphorylation of β-catenin at tyrosine residue 142 correlates with an increase in nuclear β-catenin-dependent gene expression (24). In the absence of SIRT2, we found that phospho-β-catenin Y142 is significantly elevated (Fig. 1D). Taken together, these results indicate that there is more nuclear, transcriptionally active β-catenin present in *Sirt2* KO MEFs.

SIRT2 Interacts with β-Catenin

To determine whether SIRT2 interacts with β-catenin, we performed co-immunoprecipitation experiments using cell lysates from *Sirt2* WT MEFs (Fig. 2A). SIRT2 antibody readily immunoprecipitates β-catenin (lane 2) as detected by immunoblot analysis with β-catenin antibody. In contrast, rabbit IgG does not immunoprecipitate β-catenin (lane 1), confirming the specificity of the pull down. The interaction of SIRT2 with β-catenin is also present in PC-3 cells, a human prostate adenocarcinoma cell line that endogenously expresses SIRT2 (Fig. 2B). Additionally, we overexpressed Flag-*SIRT2* or empty vector pcDNA3 in U87 glioblastoma cell line which expresses low levels of SIRT2 (Fig. 2C). Anti-Flag pull down and β-catenin immunoblot analysis demonstrates a positive interaction between Flag-SIRT2 and β-catenin which is not detected in the empty vector pcDNA3 cells.

To test whether the association between SIRT2 and β-catenin can be modulated, we exposed *Sirt2* WT MEFs to IR at 2 Gy, 5 Gy or 10 Gy delivered as a single dose before performing co-immunoprecipitation experiments (Fig. 2A). We observe that binding of SIRT2 to β-

catenin significantly increases in response to radiation (lanes 3–5) compared to unirradiated samples (lane 2), indicating the interaction is not static and can be regulated. The level of β-catenin remains constant between unirradiated (Fig. 2A, lower panel, lane 1) *vs.* irradiated samples (Fig. 2A, lower panel, lanes 2–4), confirming that the enhanced interaction between SIRT2 and β-catenin is not artifact secondary to a change in total β-catenin levels.

ROS are a well-known by-product of IR exposure, and ROS levels correlate to DNA damage that ultimately leads to cell mortality. We examined the differences in ROS levels in the presence and absence of SIRT2 at baseline and following a single exposure to 10 Gy (Fig. 2D). The level of ROS increases following IR exposure in the presence and absence of SIRT2 to a similar extent ($p = 0.054$). Interestingly, the addition of pegylated catalase (PEG-cat) was able to quench the generation of ROS in the *Sirt2* KO MEFs, but not in *Sirt2* WT.

To determine whether PEG-cat is capable of protecting the cells from IR-induced cell death by scavenging H_2O_2, we performed clonogenic survival assays using *Sirt2* WT and KO MEFs. Cells were pretreated with 200U/ml PEG-cat prior to exposure with 6 Gy radiation. As shown in Fig. 2E, without PEG-cat pretreatment, *Sirt2* KO cells were significantly more resistant to IR-induced cytotoxicity than *Sirt2* WT cells. The addition of PEG-cat did not affect the survival of *Sirt2* WT cells, but slightly increased cell survival of *Sirt2* KO cells upon radiation treatment. Therefore, these data suggest that while both *Sirt2* WT and KO cells have increased ROS upon IR exposure, *Sirt2* KO cells are more capable of handling the ROS level than *Sirt2* WT cells resulting in increased cellular survival following radiation exposure.

β-catenin is acetylated and the Wnt signaling pathway is activated in Sirt2 KO MEFs

Acetylated β-catenin has been shown to play a role in oncogenesis due to increasing β-catenin/TCF transcriptional activity (25, 26). Firestein *et al*. showed that deacetylation of β-catenin by SIRT1 can suppress colon tumorigenesis (27). To determine whether there is a difference in the level of acetylated β-catenin, *Sirt2* WT and KO MEFs were subjected to immunofluorescence staining with acetylated β-catenin antibody (Fig. 3A). Indeed, there is markedly more nuclear acetylated β-catenin present in the *Sirt2* KO MEFs compared to WT, suggesting that SIRT2 in the WT MEFs deacetylates β-catenin, giving rise to a lower level of acetylated β-catenin immunoreactivity. Concomitantly, coimmunoprecipitation experiments were also carried out using *Sirt2* WT and KO MEFs. Whole cell lysates were immunoprecipitated with β-catenin antibody and immunoblotted with either acetylated lysine or acetylated β-catenin antibody (Fig. 3B). Acetylated β-catenin is present in the *Sirt2* KO MEFs (lane 4, Ac-K and Ac-βcat panels) but not in WT. Furthermore, Flag-*SIRT2* expression in U87 glioma abolishes the acetylation of β-catenin (Fig. 3B, lane 8, Ac-K and Ac-βcat panels) further confirming that SIRT2 is responsible for deacetylating β-catenin.

To verify that SIRT2 directly deacetylates β-catenin, we performed *in vitro* deacetylation assays with β-catenin in the presence or absence of purified recombinant SIRT2 and with or without the addition of NAD+. β-catenin from *Sirt2* KO MEFs was used because it is highly acetylated as compared to β-catenin from WT MEFs (Fig. 3B). Consistent with the result in Fig. 3B, without the addition of SIRT2, β-catenin is strongly acetylated (Fig. 3C, lane 2). However, in the presence of purified recombinant SIRT2, acetylation of β-catenin was

greatly diminished (Fig. 3C, lanes 3 and 4). Interestingly, even without the addition of NAD + to the reaction, SIRT2 was able to deacetylate β-catenin fully (Fig. 3C, lane 3). We hypothesized that because we used whole cell lysates as the source of acetylated β-catenin, the pull down may also contain endogenous NAD+ that can serve as cofactor for the purified recombinant SIRT2. Exogenous NAD+ added to the reaction mixture may overwhelm the system and slow down the enzymatic activity of recombinant SIRT2, thus decreasing β-catenin deacetylation (Fig. 3C, lane 4).

GSK3β is a negative upstream regulator of β-catenin in the Wnt pathway. When the Wnt signaling pathway is in the off state, phosphorylation of β-catenin by GSK3β leads to ubiquitination and proteasomal degradation. Activation of the Wnt pathway inhibits GSK3β, allowing β-catenin to accumulate and translocate into the nucleus to turn on gene expression (2). Since there appears to be increased “active”, acetylated β-catenin in *Sirt2* KO MEFs relative to WT MEFs, we decided to evaluate the protein level of GSK3β and phosphorylated GSK3β (pGSK3β) in the 2 cell types (Fig. 3D). Although the total amount of GSK3β is similar with no significant difference between *Sirt2* WT and KO MEFs (Fig. 3D; lower panel), there is clear upregulation of pGSK3β in *Sirt2* KO cells (Fig. 3D; upper panel). Therefore, it appears that a loss of SIRT2 activates the Wnt pathway in non-transformed cells.

Downstream Wnt Target Gene Expression Is Increased in SIRT2 KO MEFs

Given that loss of SIRT2 was demonstrated to activate the Wnt pathway, we investigated whether genomic loss and knockdown of endogenously expressed *Sirt2* produced an effect on the expression of Wnt target genes. To address this question, we used a commercially-available Wnt Pathway PCR Array (Qiagen) to identify Wnt pathway genes up-regulated or down-regulated in the *Sirt2* WT vs. KO MEFs (Supplementary Table S2). Interestingly, we observe coordinated regulation of Wnt pathway genes. For example, genes that have pro-survival functions such as *cyclin D1*, *Fosl1*, *c-Jun* and *c-Myc* along with transcriptional coactivators of the Wnt pathway such as *Lef-1* and *Tcf-7* are up-regulated in *Sirt2* KO MEFs relative to WT. In contrast, genes that are negative regulators of the Wnt pathway such as *Pitx2*, *Nkd1*, *Sfrp1*, *Sfrp4 and Tle1* are down-regulated in the *Sirt2* KO MEFs compared to WT. For further studies, we decided to focus on the pro-survival genes. Additional experiments using real-time PCR confirmed increased mRNA expression of *c-myc*, *cyclin D1* and *survivin* in *Sirt2* KO cells (Fig. 4A). Similarly, immunoblot analysis revealed elevated Wnt target gene expression for c-myc, c-jun, survivin, and cyclin D1 in *Sirt2* KO MEFs (Fig. 4B). Knockdown of endogenous *Sirt2* in *Sirt2* WT MEFs using shRNA also produced increases in cyclin D1, c-myc, and survivin by real-time PCR (Fig. 4C) and immunoblot analysis (Fig. 4D). Taken together, loss of SIRT2 either by genomic deletion or shRNA inhibition results in elevated expression of Wnt target genes.

SIRT2 Represses β-catenin Transcriptional Activity

To verify that increased expression of Wnt target genes in the absence of SIRT2 occurs at the transcriptional level, we examined the effect of SIRT2 on β-catenin-mediated transcription using TOPFLASH luciferase reporter analysis (Fig. 5A). We observed that

deletion of *Sirt2* results in more than 2 fold increase in luciferase activity, suggesting transcriptional activation of the promoter containing TCF-binding sites.

Furthermore, we examined the effect of SIRT2 on the recruitment of β-catenin to TCF-binding sites of Wnt target genes by ChIP (Fig. 5B). Indeed, ChIP showed an increase in β-catenin DNA-binding activity to the *cyclin D1, c-Myc* and *survivin* promoters in *Sirt2* KO MEFs compared to WT. Increased DNA-binding to the Wnt target promoters in the absence of SIRT2 matches the increased expression of Wnt target genes. Taken together, the data suggest that SIRT2 acts as a repressor of transcription of Wnt target pro-survival genes.

SIRT2 Inhibits Cell Migration/Invasion

Microtubules have also been shown to be required for cell migration and tail retraction (28). SIRT2 has been shown to play a role in microtubule deacetylation (16) thereby raising the possibility that SIRT2 might regulate cell motility. We determined whether the absence or presence of SIRT2 changes the chemotactic movement and invasive property of MEFs. To investigate whether *Sirt2* WT and KO cells differ in motility, we subjected both cell lines to an assay that measured the ability of cells to migrate through pores in a PET membrane. As shown in Fig. 6, *Sirt2* KO fibroblasts migrate 2-fold faster than WT in response to serum (Fig. 6A) suggesting that SIRT2 is required to regulate cell motility. To examine the effect of SIRT2 on invasion, the cells are required to cross through a collagen layer as well as migrate through the pores of the chamber (Fig. 6B). Consistent with the migration result, the presence of SIRT2 markedly inhibited the invasion of MEFs through the collagen coating.

To further verify the effect of SIRT2 on invasive capacity, we performed invasion assays using *Sirt2* WT MEFs transfected with either scrambled shRNA or *Sirt2* shRNA. Knocking down *Sirt2* consistently increased the invasive capability of the cells in migrating through a collagen layer (Fig. 6C), thus further supporting results obtained with *Sirt2* KO MEFs.

Expression of MMP9 Is Dramatically Elevated In Sirt2 KO MEFs

Given that migration and invasion of MEFs were determined to be a SIRT2 dependent phenomenon, we examined if the capacity of the cell to invade extracellular matrix was also dependent on SIRT2. Previous studies have shown that matrix metalloproteinase-9 (MMP-9) (29, 30), both of which are important effectors of wound healing, tumor invasion and angiogenesis, have also been characterized as targets of β-catenin-dependent Wnt signaling. As shown in Figure 6D, *Mmp*-9 mRNA is markedly elevated in the *Sirt2* KO cells relative to WT (Fig. 6D). Immunoblot analysis further confirmed this increase in MMP-9 expression (Fig. 6E). Thus, the loss of SIRT2 results in increased *Mmp-9* mRNA and protein levels, and this observation is consistent with observed differences in the migratory and invasive behavior of the cells.

E-Cadherin is Decreased in Sirt2 KO MEFs

Because we observed a difference in adherence property between *Sirt2* WT and KO MEFs in culture, we investigated the effect of SIRT2 on E-cadherin expression. Immunoblot analysis for E-cadherin demonstrates reduced expression in *Sirt2* KO MEFs (Fig. 6E). Therefore, in addition to downstream targets of the Wnt pathway, the regulation of the

adherens junction protein E-cadherin is also dependent on the presence or absence of SIRT2. In summary, we have demonstrated that the loss of SIRT2 gives rise to the upregulation of pro-survival genes through the activation of β-catenin-dependent Wnt signaling. Concurrently, invasion and migratory capabilities become more prominent. MMP9 and E-cadherin may potentially act as molecular markers for cells lacking *Sirt2* in regulating cell migration/invasion. All of these events are the hallmarks of a *bona fide* malignancy and therefore support the hypothesis that SIRT2 functions as a tumor suppressor protein in response to IR in normal tissues.

DISCUSSION

Recent developments implicate SIRT2 as a major player in several diseases including cancer and neurodegenerative disorders. In this study, we describe a tumor suppressive role for SIRT2 using wild type and knockout *Sirt2* MEFs as a model. These findings support other published data that link the processes of tumor suppression and aging to SIRT2 and its interaction with the acetylome (31). We present evidence that SIRT2 interacts with β-catenin and represses β-catenin-mediated transcriptional gene activation. Upon SIRT2 inactivation by genetic deletion, this repression is lifted. We demonstrated that the level of transcriptionally active β-catenin increases significantly. This is established by two approaches. First, we showed that there is more β-catenin accumulation in the nucleus of *Sirt2* knockout MEFs by immunofluorescent staining and by subcellular fractionation while total whole cell β-catenin remains constant between wild-type and *Sirt2* knockout MEFs. Second, we observed that there is an increase in phospho-β-catenin Y142 as well as an increase in acetylated β-catenin level in the *Sirt2* knockout MEFs. Previous studies have shown that the phosphorylated Y142 form and acetylated form of β-catenin have increased transcriptional activity.

In accordance with increased active β-catenin in the absence of SIRT2, we showed that TCF/LEF transcription factor activity increased. Furthermore, ChIP analysis demonstrated that the presence of SIRT2 significantly attenuates β-catenin's binding to upstream promoter regions of *Myc*, *cyclin D1* and *survivin*. These findings correlate with observations that both message and protein levels of these targets are significantly elevated. Concurrently, we also showed that SIRT2 has a significant inhibitory effect on cell migration and invasion abilities. The apparent increase in invasive and migratory potential when SIRT2 is absent may be due to increased expression of MMP-9 and decreased expression of E-cadherin.

Our findings place SIRT2 as the second sirtuin to interact with β-catenin and regulate its transcriptional activity. Firestein *et al* have shown that SIRT1 plays a major role in inhibiting tumorigenesis and colon cancer growth by inhibiting β-catenin transcriptional activity *via* deacetylation (27). Similar to Firestein *et al*, we observe a difference in β-catenin acetylation between our *Sirt2* WT and KO MEFs. We presented evidence that SIRT2 interacts with β-catenin, deacetylates and suppresses β-catenin from becoming active. When SIRT2 is absent, β-catenin no longer binds and thus become activated. Taken together, these results strongly suggest that SIRT2 can act as a growth suppressor and mediate the response to IR-induced oxidative stress in normal, non-tranformed tissues. Indeed, we demonstrated that in the presence of SIRT2, radiation-induced H_2O_2 production was responsible for cell

death. These findings suggest that SIRT2 is critical to maintaining the homeostasis of non-transformed cells, and suggest that SIRT2 plays a significant role in mediating the cell's response to environmental stressors such as oxidative damage from IR.

Here, we connect endogenous SIRT2 to the interaction between the processes of aging, response to extracellular stress by IR exposure, de-differentiation and carcinogenesis. In contrast to Chen *et al* which demonstrated overexpression of SIRT2 to interact with β-catenin in hepatocellular carcinoma (32), this is the first description of endogenous SIRT2 acting directly on β catenin–in untransformed cells of advanced chronologic age, demonstrating the potential for greater oxidative stress by IR and ROS mimics in aging tissues, specifically aging central nervous system, where SIRT2 is the predominant sirtuin isoform. Recently, Simic *et al* demonstrated that SIRT1 may be a therapeutic target to foster mesenchymal stem cell differentiation to preserve the integrity of mesenchymal stem cell-derived tissues in aging animals (33). In contrast, this manuscript demonstrates for the first time that SIRT2 may be potentiating the damage induced by IR in untransformed aging cells and that disruption of the SIRT2-β– catenin interaction may be an endogenous therapeutic target to preserve the integrity of aging cells against exogenous stressors such as IR. More importantly, this demonstrates differential regulation of the same pathway by differing sirtuin isoforms.

Supplementary Material

Refer to Web version on PubMed Central for supplementary material.

Acknowledgments

This research was supported by the Intramural Research Program of the NIH, National Cancer Institute, Center for Cancer Research.

References

1. Logan CY, Nusse R. The Wnt signaling pathway in development and disease. Annu Rev Cell Dev Biol. 2004; 20:781–810. [PubMed: 15473860]
2. Gordon MD, Nusse R. Wnt signaling: multiple pathways, multiple receptors, and multiple transcription factors. J Biol Chem. 2006; 281(32):22429–33. [PubMed: 16793760]
3. Reya T, Clevers H. Wnt signalling in stem cells and cancer. Nature. 2005; 434(7035):843–50. [PubMed: 15829953]
4. Daniels DL, Weis WI. Beta-catenin directly displaces Groucho/TLE repressors from Tcf/Lef in Wnt-mediated transcription activation. Nat Struct Mol Biol. 2005; 12(4):364–71. [PubMed: 15768032]
5. Brack AS, Conboy MJ, Roy S, Lee M, Kuo CJ, Keller C, et al. Increased Wnt signaling during aging alters muscle stem cell fate and increases fibrosis. Science. 2007; 317(5839):807–10. [PubMed: 17690295]
6. Liu H, Fergusson MM, Castilho RM, Liu J, Cao L, Chen J, et al. Augmented Wnt signaling in a mammalian model of accelerated aging. Science. 2007; 317(5839):803–6. [PubMed: 17690294]
7. Ye F, Chen Y, Hoang T, Montgomery RL, Zhao XH, Bu H, et al. HDAC1 and HDAC2 regulate oligodendrocyte differentiation by disrupting the beta-catenin-TCF interaction. Nat Neurosci. 2009; 12(7):829–38. [PubMed: 19503085]
8. Toledo EM, Colombres M, Inestrosa NC. Wnt signaling in neuroprotection and stem cell differentiation. Prog Neurobiol. 2008; 86(3):281–96. [PubMed: 18786602]

9. Moon RT, Kohn AD, De Ferrari GV, Kaykas A. WNT and beta-catenin signalling: diseases and therapies. Nat Rev Genet. 2004; 5(9):691–701. [PubMed: 15372092]
10. Yao H, Ashihara E, Maekawa T. Targeting the Wnt/beta-catenin signaling pathway in human cancers. Expert Opin Ther Targets. 2011
11. Harting K, Knoll B. SIRT2-mediated protein deacetylation: An emerging key regulator in brain physiology and pathology. Eur J Cell Biol. 2010; 89(2–3):262–9. [PubMed: 20004495]
12. Taylor DM, Maxwell MM, Luthi-Carter R, Kazantsev AG. Biological and potential therapeutic roles of sirtuin deacetylases. Cell Mol Life Sci. 2008; 65(24):4000–18. [PubMed: 18820996]
13. Haigis MC, Sinclair DA. Mammalian sirtuins: biological insights and disease relevance. Annu Rev Pathol. 2010; 5:253–95. [PubMed: 20078221]
14. Hiratsuka M, Inoue T, Toda T, Kimura N, Shirayoshi Y, Kamitani H, et al. Proteomics-based identification of differentially expressed genes in human gliomas: down-regulation of SIRT2 gene. Biochem Biophys Res Commun. 2003; 309(3):558–66. [PubMed: 12963026]
15. Matsushita N, Takami Y, Kimura M, Tachiiri S, Ishiai M, Nakayama T, et al. Role of NAD-dependent deacetylases SIRT1 and SIRT2 in radiation and cisplatin-induced cell death in vertebrate cells. Genes Cells. 2005; 10(4):321–32. [PubMed: 15773895]
16. Tang BL, Chua CE. SIRT2, tubulin deacetylation, and oligodendroglia differentiation. Cell Motil Cytoskeleton. 2008; 65(3):179–82. [PubMed: 18044719]
17. Maxwell MM, Tomkinson EM, Nobles J, Wizeman JW, Amore AM, Quinti L, et al. The Sirtuin 2 microtubule deacetylase is an abundant neuronal protein that accumulates in the aging CNS. Hum Mol Genet. 2011; 20(20):3986–96. [PubMed: 21791548]
18. Kim HS, Vassilopoulos A, Wang RH, Lahusen T, Xiao Z, Xu X, et al. SIRT2 maintains genome integrity and suppresses tumorigenesis through regulating APC/C activity. Cancer Cell. 2011; 20(4):487–99. [PubMed: 22014574]
19. Mushinski JF, Nguyen P, Stevens LM, Khanna C, Lee S, Chung EJ, et al. Inhibition of tumor cell motility by the interferon-inducible GTPase MxA. J Biol Chem. 2009; 284(22):15206–14. [PubMed: 19297326]
20. Nguyen P, Bar-Sela G, Sun L, Bisht KS, Cui H, Kohn E, et al. BAT3 and SET1A form a complex with CTCFL/BORIS to modulate H3K4 histone dimethylation and gene expression. Mol Cell Biol. 2008; 28(21):6720–9. [PubMed: 18765639]
21. Slane BG, Aykin-Burns N, Smith BJ, Kalen AL, Goswami PC, Domann FE, et al. Mutation of succinate dehydrogenase subunit C results in increased O2 -, oxidative stress, and genomic instability. Cancer Res. 2006; 66(15):7615–20. [PubMed: 16885361]
22. Zhang Y, Zhang M, Dong H, Yong S, Li X, Olashaw N, et al. Deacetylation of cortactin by SIRT1 promotes cell migration. Oncogene. 2009; 28(3):445–60. [PubMed: 18850005]
23. Isaacs JS, Jung YJ, Mole DR, Lee S, Torres-Cabala C, Chung YL, et al. HIF overexpression correlates with biallelic loss of fumarate hydratase in renal cancer: novel role of fumarate in regulation of HIF stability. Cancer Cell. 2005; 8(2):143–53. [PubMed: 16098467]
24. Brembeck FH, Rosario M, Birchmeier W. Balancing cell adhesion and Wnt signaling, the key role of beta-catenin. Curr Opin Genet Dev. 2006; 16(1):51–9. [PubMed: 16377174]
25. Levy L, Wei Y, Labalette C, Wu Y, Renard CA, Buendia MA, et al. Acetylation of beta-catenin by p300 regulates beta-catenin-Tcf4 interaction. Mol Cell Biol. 2004; 24(8):3404–14. [PubMed: 15060161]
26. Xu W, Kimelman D. Mechanistic insights from structural studies of beta-catenin and its binding partners. J Cell Sci. 2007; 120(Pt 19):3337–44. [PubMed: 17881495]
27. Firestein R, Blander G, Michan S, Oberdoerffer P, Ogino S, Campbell J, et al. The SIRT1 deacetylase suppresses intestinal tumorigenesis and colon cancer growth. PLoS One. 2008; 3(4):e2020. [PubMed: 18414679]
28. Ballestrem C, Wehrle-Haller B, Hinz B, Imhof BA. Actin-dependent lamellipodia formation and microtubule-dependent tail retraction control-directed cell migration. Mol Biol Cell. 2000; 11(9): 2999–3012. [PubMed: 10982396]
29. Crawford HC, Fingleton BM, Rudolph-Owen LA, Goss KJ, Rubinfeld B, Polakis P, et al. The metalloproteinase matrilysin is a target of beta-catenin transactivation in intestinal tumors. Oncogene. 1999; 18(18):2883–91. [PubMed: 10362259]

30. Wu B, Crampton SP, Hughes CC. Wnt signaling induces matrix metalloproteinase expression and regulates T cell transmigration. Immunity. 2007; 26(2):227–39. [PubMed: 17306568]

31. Park SH, Zhu Y, Ozden O, Kim HS, Jiang H, Deng CX, et al. SIRT2 is a tumor suppressor that connects aging, acetylome, cell cycle signaling, and carcinogenesis. Transl Cancer Res. 2012; 1(1):15–21. [PubMed: 22943040]

32. Chen J, Chan AW, To KF, Chen W, Zhang Z, Ren J, et al. SIRT2 overexpression in hepatocellular carcinoma mediates epithelial to mesenchymal transition via akt/GSK-3beta/beta-catenin signaling (revised version). Hepatology. 2013

33. Simic P, Zainabadi K, Bell E, Sykes DB, Saez B, Lotinun S, et al. SIRT1 regulates differentiation of mesenchymal stem cells by deacetylating beta-catenin. EMBO Mol Med. 2013; 5(3):430–40. [PubMed: 23364955]

Implications

Disruption of the SIRT2/β-catenin interaction represents an endogenous therapeutic target to prevent transformation and preserve the integrity of aging cells against exogenous stressors such as reactive oxygen species.

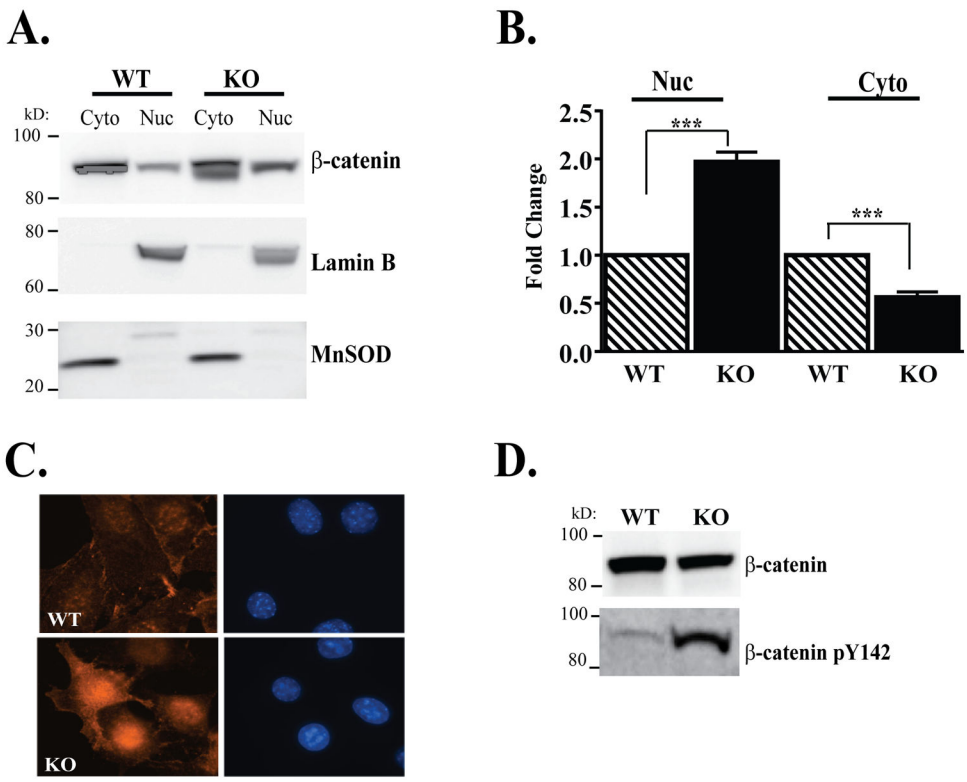

Figure 1.

Nuclear β-catenin levels are elevated in *Sirt2* KO MEFs. A, immunoblot analysis of enriched nuclear and cytoplasmic fractions for β-catenin, lamin B (nuclear marker) or manganese superoxide dismutase (cytoplasmic marker) showing increased nuclear β-catenin protein level in *Sirt2* KO MEFs. B, densitometric analysis of the subcellular fractionation. ***, $P < 0.001$. C, immunoblot analysis showing increased pY142 β-catenin in *Sirt2* KO MEFs. D, β-catenin immunofluoresescent staining showing markedly increased level of nuclear β-catenin in *Sirt2* KO MEFs vs. WT.

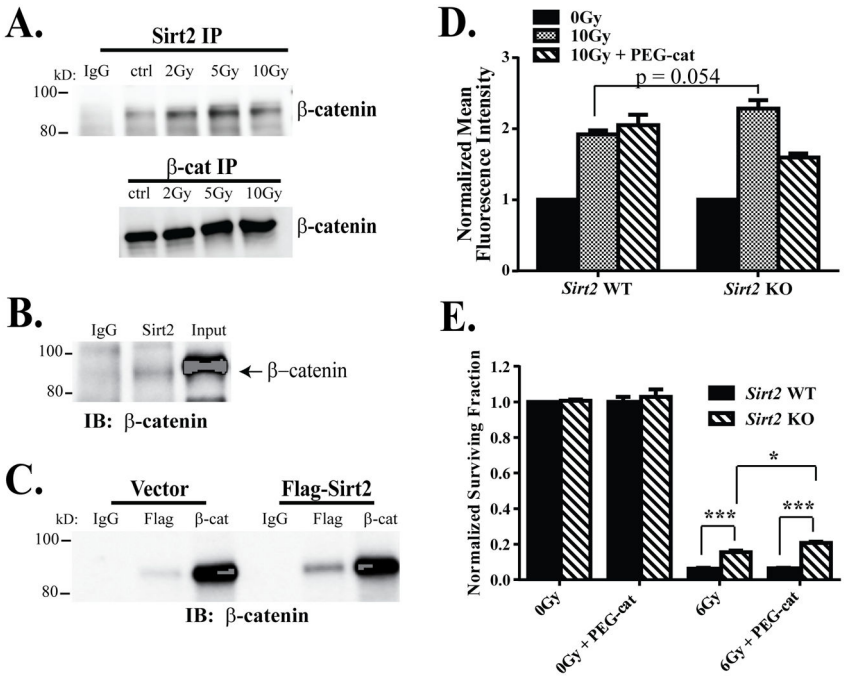

Figure 2.

SIRT2 interacts directly with β-catenin. A, coimmunoprecipitation showing association of SIRT2 and β-catenin increases with IR. *Sirt2* WT MEFs were exposed to single fractions of 2Gy, 5 Gy and 10 Gy, and compared to sham controls. Cells were harvested 24h after radiation and immunoprecipitated either with normal rabbit IgG control, SIRT2 or β-catenin antibodies. Bound proteins were analyzed by immunoblot with β-catenin antibody. B, coimmunoprecipitation analysis showing SIRT2 associates with β-catenin in PC-3 cells. C, coimmunoprecipitation analysis showing overexpressed Flag-SIRT2 binds to β-catenin. Protein lysates from U87 glioma cells stably expressing either pcDNA3 or Flag-*SIRT2* were subjected to immunoprecipitation using rabbit IgG, DDK or β-catenin antibodies. Bound proteins were analyzed by immunoblot with β-catenin antibody. D, ROS measurement. *Sirt2* WT and KO MEFs were labeled with H_2DCFDA or carboxy DCFDA for 30 min before exposure to a single fraction of 10 Gy compared to sham controls. Cells were harvested after 30 min and analyzed. Treatment with PEG-catalase was used to scavenge ROS generated by radiation. E, Clonogenic survival assay. *Sirt2* WT and KO cells were plated for clonogenic survival assay and treated with 200U/ml PEG-cat for 2h, followed by radiation. PEG-cat was left for the duration of the assay. Values represent the mean +/− SEM. *, $P < 0.05$, ***, $P < 0.005$

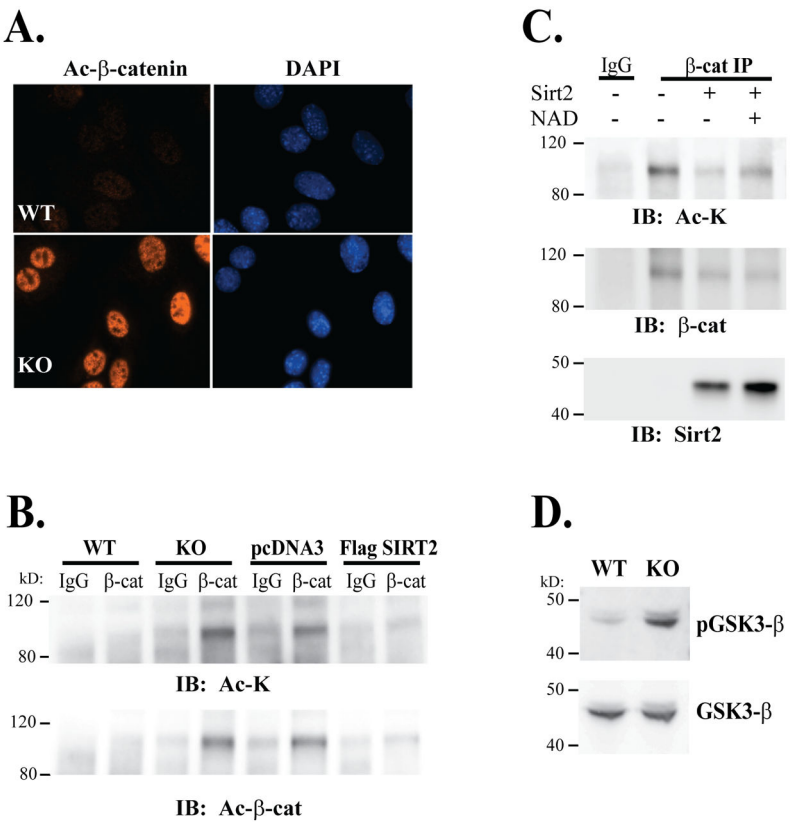

Figure 3.

Acetylation of β-catenin and activation of the Wnt signaling pathway in *Sirt2* KO MEFs. A, acetylated β-catenin immunofluorescent staining showing markedly increased level of acetylated β-catenin present in *Sirt2* KO MEFs compared to WT. B, increased acetylated β-catenin is present in *Sirt2* KO MEFs. Whole cell lysates from *Sirt2* WT and KO cells were immunoprecipitated with rabbit IgG control or β-catenin antibody. Pulled-down complexes were immunoblotted with acetylated lysine or acetylated β-catenin antibody. C, SIRT2 deacetylates β-catenin *in vitro*. Immunoprecipitated β-catenin from Sirt2 KO MEFs was incubated with or without purified recombinant Sirt2 in the presence or absence of NAD+. The reaction mixtures were separated by SDS-PAGE and immunoblotted with antibodies against acetylated lysine, β-catenin or SIRT2. D, immunoblot showing upregulated level of activated, phosphorylated GSK-3-β in *Sirt2* KO MEFs compared to WT.

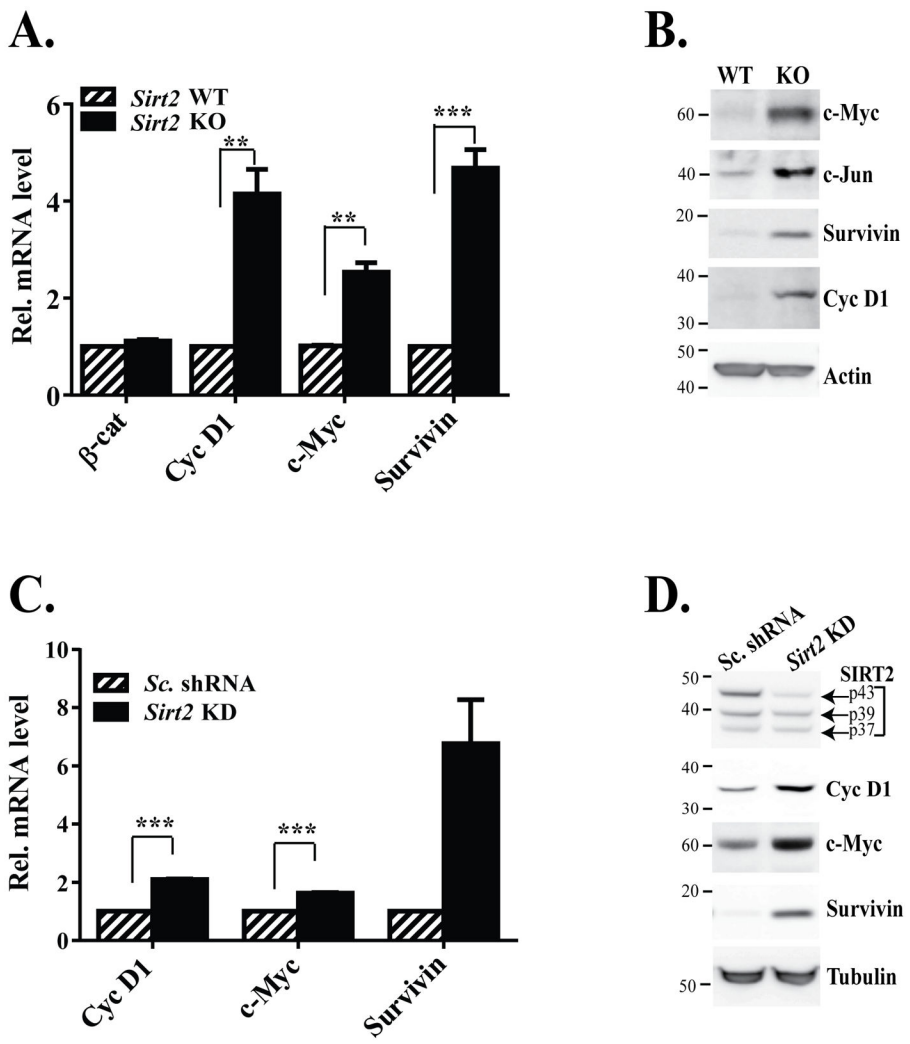

Figure 4.

SIRT2 inhibits Wnt target gene expression. A, real-time PCR showing upregulated mRNA levels of *cyclin D1*, *c-myc* and *survivin* in *Sirt2* KO MEFs compared with WT. **, P < 0.005, ***, P < 0.0005. B, immunoblot showing increased protein levels of c-myc, cyclin D1, survivin and c-Jun in *Sirt2* KO compared to WT. C, real-time PCR showing that knockdown of *Sirt2* upregulates *cyclin D1*, *c-myc* and *survivin* mRNA levels. ***, P < 0.001. D, immunoblot showing knockdown of *Sirt2* upregulates c-myc, cyclin D1 and survivin protein expression.

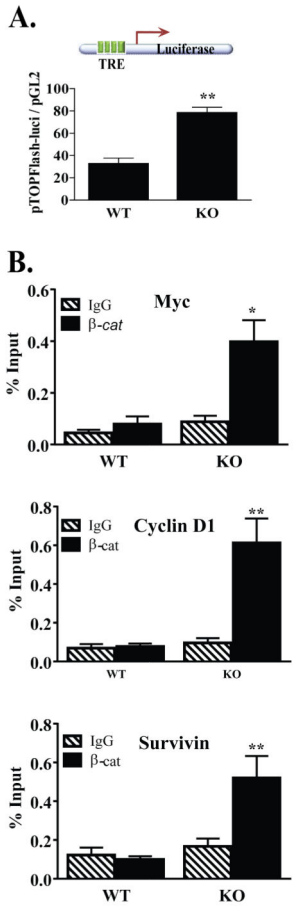

Figure 5.

SIRT2 inhibits Wnt Signaling. A, pTOPFLASH luciferase promoter analysis showing upregulated TCF/LEF transcriptional activity in *Sirt2* KO MEFs compared to WT. **, $P < 0.005$. B, ChIP analysis showing increased binding of β-catenin to the promoters of *c-myc*, *cyclin D1*, and *survivin*. *, $P < 0.5$, **, $P < 0.01$.

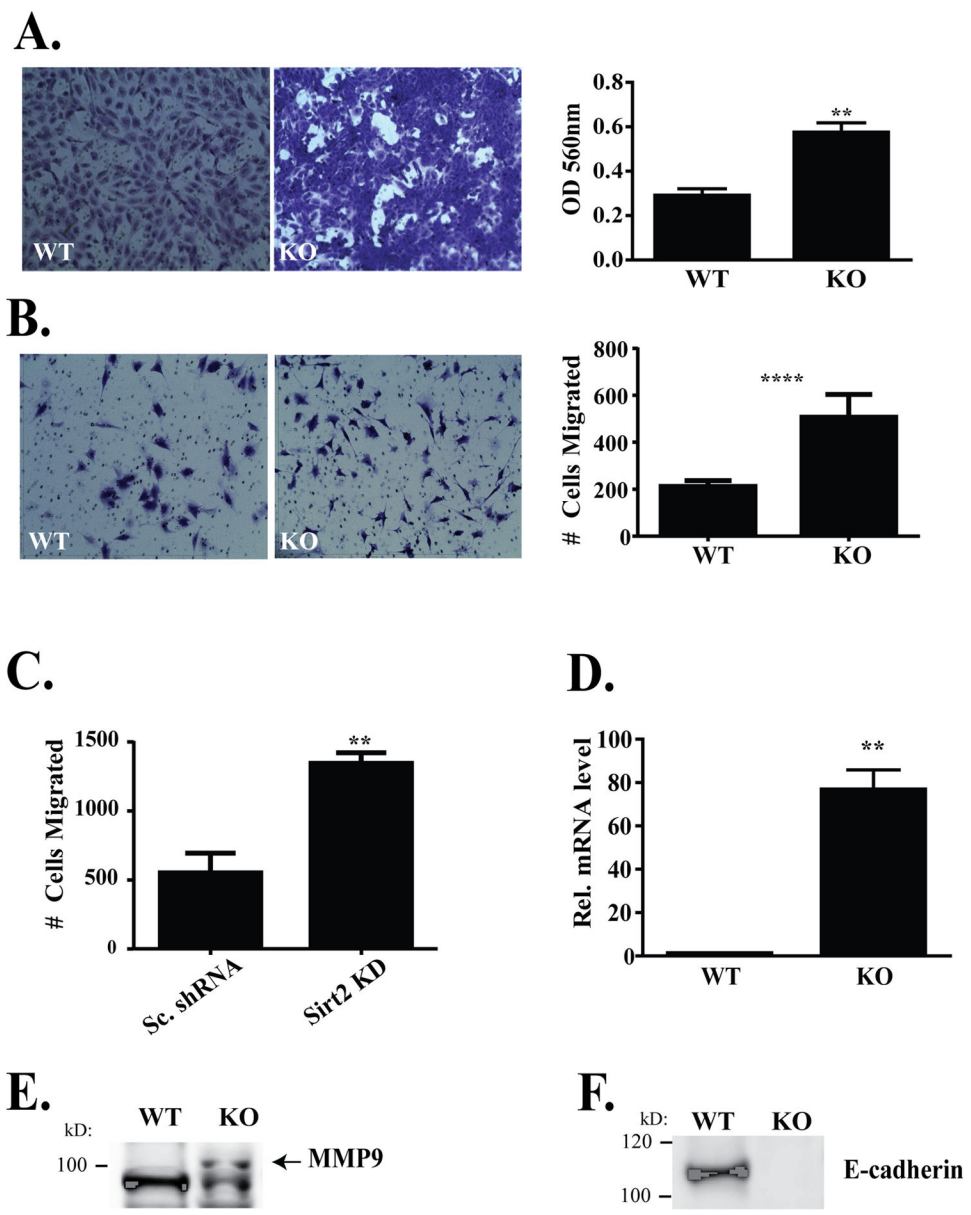

Figure 6.

SIRT2 inhibits cell motility/invasion and MMP9 expression and upregulates E-cadherin expression. A, cell motility analysis showing *Sirt2* KO MEFs migrated faster through uncoated Boyden chambers compared to WT in response to serum. B, cell invasion analysis showing *Sirt2* KO fibroblasts migrated faster through collagen-coated Boyden chambers in response to serum. ***, P < 0.0001. C, cell invasion analysis showing that knockdown of *Sirt2* slowed the migration of *Sirt2* WT MEFs through collagen-coated Boyden chambers. **, P,< 0.005. D, real-time PCR showing upregulated *Mmp9* mRNA in *Sirt2* KO MEFs compared to WT. **, P < 0.005. E, immunoblot showing increased MMP9 in *Sirt2* KO cells compared to WT. F, immunoblot showing markedly decreased E-cadherin in *Sirt2* KO cells compared to WT. Data from A–C in this figure are representative of one of three

independent experiments. Data from D–F in this figure show means ± SEM from three independent experiments.